

Gd anchored Bismuth Ferrite: Investigations on Structural and Optical Properties

Sourabh Sharma^a, Sonia^b, Harita Kumari^c, Ashok Kumar^{b*} & O P Thakur^a

^aDepartment of Physics, Materials Analysis and Research Laboratory, NSUT, Dwarka, New Delhi 110 078, India

^bDepartment of Physics, Deenbandhu Chhotu Ram University of Science and Technology, Murthal, Haryana 131 039, India

^cDepartment of Physics, Maharshi Dayanand University, Rohtak, Haryana 124 001, India

Received 9 July 2023; accepted 14 August 2023

The potential of rare-earth doping to robust structural, magnetic, electric, and optical characteristics of bismuth ferrite (BFO) has prompted an enormous amount of interest in the field of materials science. Gd-substituted BFO were produced in this work utilizing Pechini's modified Sol-Gel auto combustion technique. The development of a pure perovskite structure was confirmed by X-ray diffraction (XRD), with no secondary phases identified. The lattice parameters were observed to decrease as Gd concentration increased, showing that Gd ions were successfully incorporated into the BFO lattice. The microstructural characteristics of the produced NPs were investigated using the HRTEM to evaluate particle size and shape. UV-Vis spectroscopy was used to analyze the optical characteristics of the NPs, which revealed a reduction in optical bandgap with Gd substitution. The improved optical characteristics can be attributed to a change in the electronic band structure caused by Gd substitution. Overall, Gd-substituted BFO perovskites displays remarkable optical properties, indicating their potential use in optoelectronic devices and as a catalyst for the degradation of synthetic and organic dyes.

Keywords: Rare-earth doping; Sol-Gel auto combustion technique; Perovskites; Optoelectronic properties

1 Introduction

In recent years, rare-earth modified bismuth ferrite (BFO) has become a captivating material due to its potential for enhancing the structural, magnetic, electric, and optical properties of BFO. As a multiferroic material, bismuth ferrite possesses both ferroelectric and antiferromagnetic properties, making it a promising candidate for applications including spintronics, data storage, and sensors. However, the inherent limitations of pure BFO, such as its relatively large bandgap and low photovoltaic efficiency, have prompted considerable research interest in modifying its properties via rare earth substitution^{1,2}.

This article examines the structural and optical characteristics of Gd-modified BFO. Gadolinium, a rare earth element, possesses distinctive properties that can be utilized to modify the properties of BFO. The introduction of Gd ions into the BFO lattice can alter the crystal structure, bandgap, and optical absorption properties of the material. By comprehending and identifying these modifications, researchers can gain insight into the underlying mechanisms and refine the material for particular applications^{3,4}.

The investigation of Gd-modified BFO involves a comprehensive analysis employing techniques such as X-ray diffraction (XRD) (Rikagu ultima IV) for structural characterization, High-Resolution Transmission Electron Microscopy (HRTEM) (TEI Technai TF-20), UV-Vis spectroscopy (UV-3600 I plus Serial no. – A126158 SHIMADZU) for optical absorption studies.

This article presents a systematic investigation into the structural and optical properties of Gd-modified BFO at various doping concentrations. The obtained results will cast light on the structural modifications induced by Gd substitution and their subsequent effect on the optical properties. These discoveries can pave the way for the creation of BFO-based materials with improved performance in photocatalysis, optoelectronic devices, and other technological applications.

2 Materials and Methods

Pechini's modified sol-gel auto-combustion route is used to synthesize the nanoparticles of gadolinium-substituted bismuth ferrite ($\text{Bi}_{1-x}\text{Gd}_x\text{FeO}_3$, $x = 0.0, 0.05, 0.10, 0.15, 0.20$). The synthesis started with $\text{Bi}(\text{NO}_3)_3 \cdot 5\text{H}_2\text{O}$ (SRL, Purity 98.5%), $\text{Fe}(\text{NO}_3)_3 \cdot 9\text{H}_2\text{O}$ SRL, (98%), and $\text{Gd}(\text{NO}_3)_3 \cdot 5\text{H}_2\text{O}$ SRL, (99.9%). The magnetic stirrer dissolves them in 20 ml

*Corresponding authors: (E-mail: ashokkumar.phy@dcrustm.org)

of distilled water in separate beakers for 15 minutes. All the homogeneous solutions are then poured using burette, into a beaker containing 50 ml distilled water. As a chelating agent, 8-9 grams of anhydrous Citric acid ($C_6H_8O_7$) is added to the solution. 25% Liq. NH_3 is added to raise pH to 7. After that, the hot plate magnetic stirrer was heated to 80 degrees Celsius and swirled for four to five hours until the liquid formed into a thick resin or gel.

The gel is formed, the temperature of hot plate was raised to 300 °C to start the auto-combustion process, producing a fluffy powder that was pulverized in an agate mortar and pestle. Gd-substituted BFO nanoparticles were annealed in a muffle furnace at 600 °C for 6 hours at a constant heating rate of 5 °C/min.

2.1 XRD Analysis

To study the structural effects of Gd substitution on $Bi_{1-x}Gd_xFeO_3$ ($x = 0.0, 0.05, 0.10, 0.15, 0.20$) NPs, the XRD patterns are analyzed which are shown in Fig. 1.

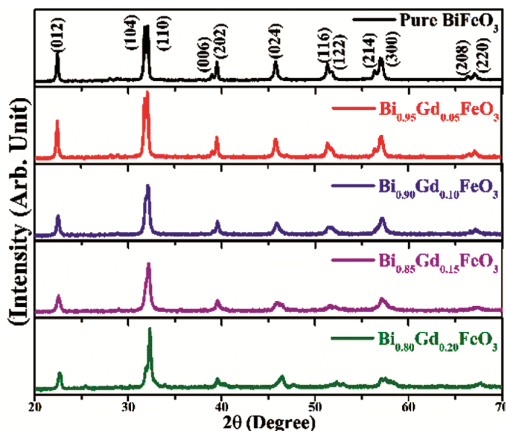


Fig. 1 — XRD patterns of $Bi_{1-x}Gd_xFeO_3$ ($x = 0.0, 0.05, 0.10, 0.15, 0.20$) NPs (JCPDS No. 74-2493).

The patterns confirm the crystallinity and single-phase (R3c space group) structure of the synthesized NPs. Gd doping significantly affected crystallite size, dislocation density, and lattice properties, according to the XRD patterns. With increase in the concentration of Gd ions, the crystallite size and particle size decreases. Gd ions in the BFO lattice disrupts the crystal structure, preventing bigger crystallites from growing. Gd concentration decreased dislocation density, according to XRD analysis. Doped NPs have more structural order than undoped BFO because their dislocation density is lower. Gd ions replacing Bi ions in the BFO structure constrict the crystal lattice. The compacted crystal lattice is due to Gd's lower ionic radius than Bi. The structural parameters such as crystallite size (D), dislocation density (δ^2), and lattice parameters were calculated by using the XRD data which is written in Table 1.

2.2 HRTEM Analysis

To determine how Gd substitution affects particle size, $Bi_{1-x}Gd_xFeO_3$ nanoparticles ($x = 0.0, 0.05, 0.10, 0.15, 0.20$) were analyzed by HRTEM. The HRTEM images of crystalline NPs is given in Fig. 2. With increasing Gd concentration the particle size of

Table 1 — Structural parameters calculated by using XRD data

| Sample | D(nm) | δ^2 | a=b(Å) | c(Å) |
|---------------------------|-------|------------|--------|-------|
| $BiFeO_3$ | 23 | 0.0018 | 5.57 | 13.69 |
| $Bi_{0.95}Gd_{0.05}FeO_3$ | 21 | 0.0022 | 5.57 | 13.71 |
| $Bi_{0.90}Gd_{0.10}FeO_3$ | 18 | 0.0030 | 5.56 | 13.77 |
| $Bi_{0.85}Gd_{0.15}FeO_3$ | 13 | 0.0059 | 5.53 | 13.77 |
| $Bi_{0.80}Gd_{0.20}FeO_3$ | 17 | 0.0034 | 5.51 | 13.79 |

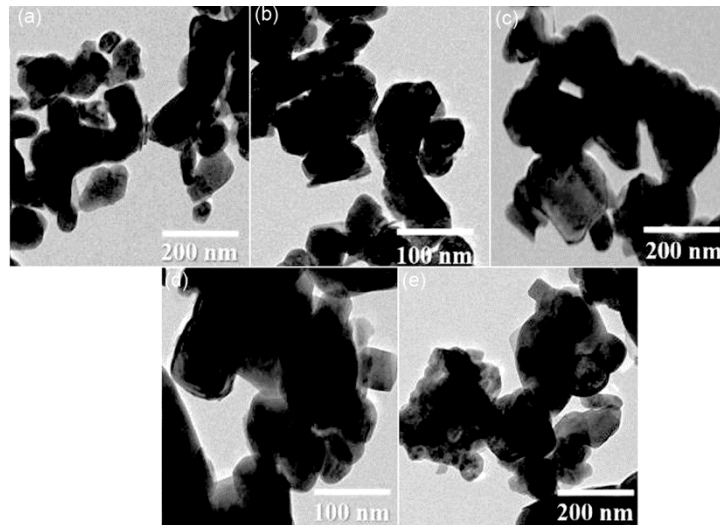


Fig. 2 — (a)-(e) HRTEM images of $Bi_{1-x}Gd_xFeO_3$ ($x = 0.0, 0.05, 0.10, 0.15, 0.20$) NPs respectively.

produced NPs decreases. Undoped BFO nanoparticles had greater particle sizes, indicating agglomerations and bigger crystalline domains. Particle size decreased with Gd concentration from $x = 0.05$ to 0.20 . Gd ions in the BFO lattice may slow down the crystal development, resulting in smaller nanoparticles.

Particle size reduction can affect material characteristics and uses. With decreasing particle size, surface area to volume ratio increases and this increased surface area-to- volume ratio can increase catalytic activity, sensing, and optical characteristics in nanoparticles. HRTEM study revealed Gd-substituted NPs shape and structure⁵. The photos showed well-defined structures, proving the nanoparticles were single- crystalline. The particle size of the synthesized samples in well written in Table 2.

2.3 UV-Vis Spectroscopy Analysis

Tauc's plot analysis on $\text{Bi}_{1-x}\text{Gd}_x\text{FeO}_3$ ($x = 0.0, 0.05, 0.10, 0.15, 0.20$) samples examined the effects of Gd doping on the band gap. After obtaining

Table 2 — Optical band gap and particle size of respective samples

| Sample | Band gap (eV) | Particle Size (nm) |
|--|---------------|--------------------|
| BiFeO_3 | 2.12 | 70.87 |
| $\text{Bi}_{0.95}\text{Gd}_{0.05}\text{FeO}_3$ | 2.09 | 66.67 |
| $\text{Bi}_{0.90}\text{Gd}_{0.10}\text{FeO}_3$ | 2.07 | 48.21 |
| $\text{Bi}_{0.85}\text{Gd}_{0.15}\text{FeO}_3$ | 2.02 | 16.82 |
| $\text{Bi}_{0.80}\text{Gd}_{0.20}\text{FeO}_3$ | 2.00 | 67.91 |

the absorption spectra of the materials using UV-Vis spectroscopy, Tauc's plot analysis was performed. Extending the figure's linear segment to the energy axis approximates the optical band gap⁶. The band gap estimation is presented in the Fig. 3.

The Tauc's plot demonstrated that Gd substitution reduced the optical band gap. The band gap of an undoped BFO sample was 2.12 eV. The band gap decreased to 2.0 eV ($x = 0.20$) with increasing Gd concentration in the sample.

The electron transition energy gap diminishes the band gap. In the BFO lattice Gd ions alter levels of energy and the electronic structure. Smaller band gaps enhance photon absorption in the visible spectrum, thereby enhancing optoelectronics and solar energy conversion. The narrower band gap of Gd-doped BFO may aid photocatalysis in producing and utilizing charge carriers⁷. The optical band gap of the produced NPs is compared with the previously reported work in Table 3.

Table 3 — Comparison of optical band gap of previously reported studies with the present work.

| Sample | Band Gap (eV) | Application | Reference |
|--|---------------|------------------------------|------------------------------|
| $\text{Bi}_{0.9}\text{Gd}_{0.1}\text{FeO}_3$ | 1.9 | Photocatalysis | Arti et. al. ⁸ |
| $\text{Bi}_{0.9}\text{Gd}_{0.1}\text{FeO}_3$ | 2.03 | Photocatalysis | Gou et. al. ⁹ |
| $\text{Bi}_{0.95}\text{Gd}_{0.05}\text{FeO}_3$ | 2.51 | Solar cells (Proposed) | Sharma et. al. ¹⁰ |
| $\text{Bi}_{0.80}\text{Gd}_{0.2}\text{FeO}_3$ | 2.00 | Photocatalysis (Proposed) | Present work |

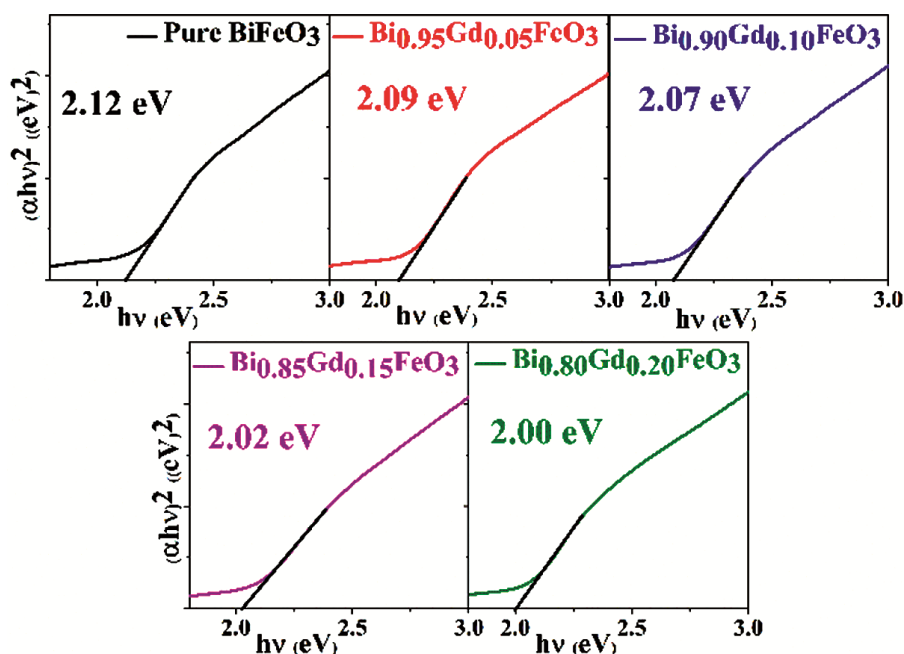


Fig. 3 — Tauc's Plot of the $\text{Bi}_{1-x}\text{Gd}_x\text{FeO}_3$ ($x = 0.0, 0.05, 0.10, 0.15, 0.20$) NPs.

3 Conclusion

In a nutshell, multiferroic rare-earth Gd-substituted bismuth ferrite was synthesized having varied conc. $\text{Bi}_{1-x}\text{Gd}_x\text{FeO}_3$ ($x = 0.0, 0.05, 0.10, 0.15, 0.20$) using sol gel auto combustion method. The patterns from XRD diffraction analysis demonstrate that the synthesized NPs are crystalline and have a single-phase structure (R3c space group) which proves Gd considerably altered crystallite size, dislocation density, and lattice characteristics. Increasing Gd doping concentration decreases the particle size due to slow crystal development, resulting in smaller nanoparticles. Gd ions alter the energy and electronic structure in BFO lattices. Smaller band gaps increase visible-spectrum photon absorption, improving optoelectronics and solar energy conversion. This tailoring of band gap can be used according to the need in various applications like photocatalysis and photo voltaic devices.

Acknowledgment

The authors acknowledge the DST-FIST lab at the department of Physics, DCRUST, Murthal for providing research and characterization facilities.

Authors would also like to thank Ms. Sweetly Dahiya for her meticulous reading and insightful critical reviews which greatly enhanced the quality of our work.

References

- 1 Sahu A K, Satpathy S K, Rout S K & Behera B, *Trans Electr Electron Mater*, 21 (2020) 217.
- 2 Rhaman M M, Matin M A, Al Mamun M A, Hussain A, Hossain M N, Das B C, Hakim M A & Islam, M F, *J Mater Sci Mater Electron*, 31 (2020) 8727.
- 3 Sheoran N, Saini M, Kumar A, Kumar V, Kumar T & Sheoran M, *MRS Adv*, 4 (2019).
- 4 Das R, Sarkar T & Mandal K, *J Phys D Appl Phys*, 45 (2012).
- 5 Pandey R, Panda C, Kumar P & Kar M, *J Sol-Gel Sci Technol*, 85 (2018) 166.
- 6 Kumar S K, Ramu S, Sudharani A, Ramanadha M, Murali G & Vijayalakshmi R P, *Phys E Low-Dimensional Syst Nanostruct*, 115 (2020)113689.
- 7 Arora M & Kumar M, *Mater Lett*, 137 (2014) 285.
- 8 Arti, Gupta R, Singh S P, Walia R, Kumar V & Verma V, *J Alloys Compd*, (2022) 908.
- 9 Guo R, Fang L, Dong W, Zheng F & Shen M, *J Phys Chem C*, 14 (2010) 21390.
- 10 Sharma A D & Sharma H B, *J Mater Sci Mater Electron*, 32 (2021) 20612.